Seed-bank contribution in maintaining phytoplanktonic biodiversity

April 30, 2020

Growth calibration

The growth function in our models can be separated in three elements:

$$N_{t',i} = \frac{\exp(E(T)f_i(T))N_{t,i}}{g(\alpha_{ij}, N_{t,j})} \tag{1}$$

with $E(T)$ being the maximum achievable growth rate, $f_i(T)$, the niche part of the model, and $g(\alpha_{ij}, N_{j,t})$, the effect of interactions on the growth rate.

This section is dedicated to the design of the growth function $E(T)$, the taxon-specific function $f_i(T)$ that characterizes differential response to temperature variations, and the estimation of interactions that may reduce it.

Common response to temperature

Phytoplanktonic growth rates cover a large range of values: between 0.2 and 1.78 day^{-1} for diatoms in Reynolds (2006), even reaching 3 day^{-1} in the meta-analysis of 308 experiments by Edwards *et al.* (2015). These values are often computed from measurements on isolated species or on limited communities in laboratory conditions, with constant environmental conditions. Gathering sets of data is therefore necessary to understand general responses to changes in the environment (Bissinger *et al.*, 2008; Edwards *et al.*, 2016). While the shape of the response may vary between taxa, the equation by Scranton & Vasseur (2016) on which we base our growth rate formulation is not able to reproduce the observed patterns (see low values of the growth rate in Fig. 1 a). In this context, we decided to use the formula by Bissinger *et al.* (2008) to compute the maximum growth rate response to the temperature. There are two reasons for this choice. First, their model is a general function that can be applied to all species. Second, Bissinger *et al.* (2008) is an update of the seminal work of Eppley (1972) used in Scranton & Vasseur (2016).

The relationship between temperature and growth rate is then $E(T) = 0.81\mathrm{e}^{0.0631T_{\circ C}}$, with $T_{\circ C}$ in Celsius degrees. In this case, growth rates vary between 0.81 and 3.9 day^{-1} for temperatures between 0 and 25°C, in line with previous observations. However, these daily growth rates need to be proportional to the daylength as no growth occurs at night: we therefore halve the Bissinger value in our models.

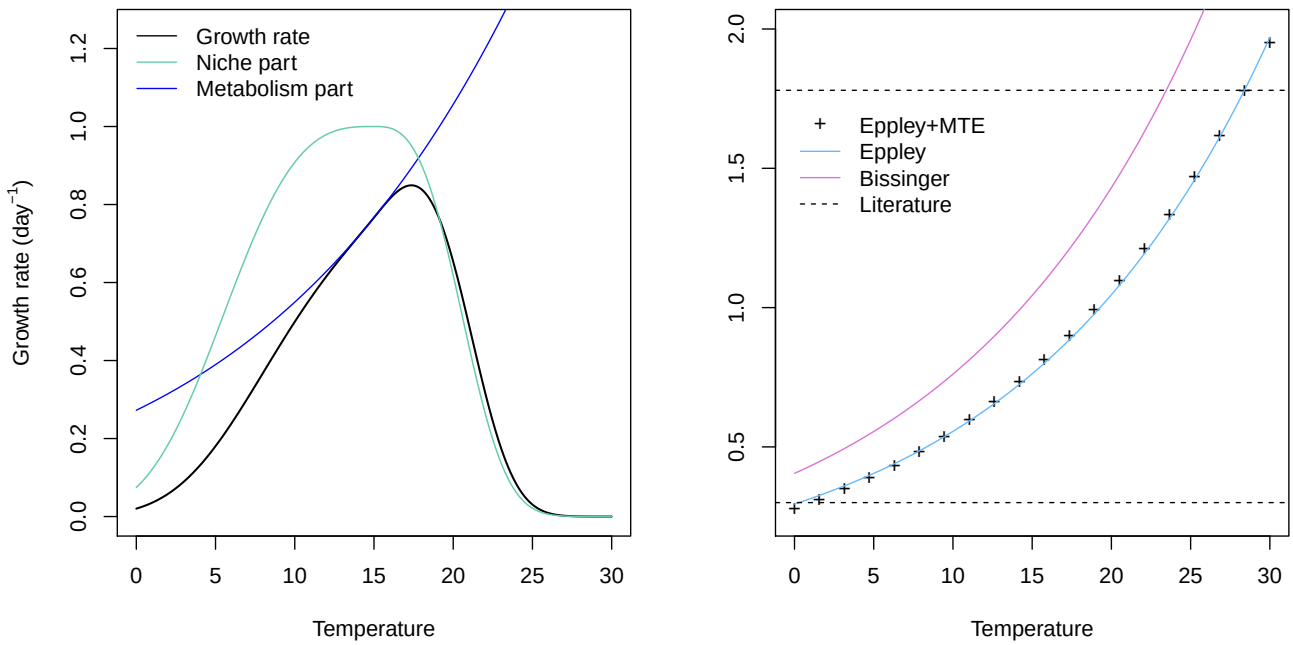

Figure 1: Decomposition of the Scranton & Vasseur (2016) growth rate formula (a). The black line indicates the final growth rate with their model. The blue line corresponds to the taxon-specific response to temperature for a thermal optimum of 15°C and the green line is the maximum achievable growth rate, a composite of the metabolic theory of ecology and the formula by Eppley (1972). This formula is shown by black crosses in (b) and compared to the Eppley (1972) curve in blue and Bissinger *et al.* (2008) formula in purple. Horizontal lines show limits found the literature (Reynolds, 2006).

Taxon-specific response to temperature

The niche part of the growth rate $f_i(T)$ is mainly defined by two parameters: the thermal optimum $T_{K,i}^{opt}$ in Kelvin and a proxy of the niche width b_i, which drive the phenology of the taxon (eq. 2).

$$f_i(T) = \begin{cases} \exp(-|T_K - T_{K,i}^{opt}|^3/b_i), & T_K \leq T_{K,i}^{opt} \\ \exp(-5|T_K - T_{K,i}^{opt}|^3/b_i), & T > T_{K,i}^{opt} \end{cases} \quad (2)$$

Each year, the dynamics of phytoplanktonic organisms is characterized by a blooming period and a lower concentration during the rest of the year. The bloom can be triggered by a combination of nutrient and light input, as well as a sufficient temperature. All parameters being more or less dependent on seasonality, it is reasonable to restrain this study to the effect of temperature.

We base estimates of $T_{K,i}^{opt}$ and b_i on field observations. For each taxon and each year, the beginning of the bloom of a given taxon is defined by the date at which its abundance exceeds its median abundance over the year. The duration of the bloom is the number of days between the beginning and the date where abundance falls below the median value. Taxa are then separated into two groups. In the field, generalists are characterized by one long bloom in the year or several blooms during which the abundances oscillate around their median. Specialists tend to appear only once or twice in the year for shorter amounts of time. A genus is therefore defined as a generalist if its cumulated blooms over a year last more than the average duration of all blooms (137 days) for at least 15 years over the 20 years of the time series, and as a specialist if they fall below this threshold.

In the models, we assume that generalists have a niche width between 15 and 30°C and specialists, between 5 and 10°C. We assume that temperatures outside of this range lead to a growth rate at least 10 times inferior to the

growth rate obtained at their thermal optimum ($\exp(-|7.5|^3/b_i = 0.1$ for a niche width of 15°C). This leads to values of b_i between 180 and 1500 for generalists, and 7 and 55 for specialists. A set of b values is drawn from a uniform distribution with these boundaries. Meanwhile, taxa are ordered as a function of the mean cumulated bloom length and larger niche values are attributed to longer mean bloom length, i.e. $\sum \overline{L}_{i,b} > \sum L_{j,b} \Rightarrow b_i > b_j$ where $\overline{L}$ is the mean over 20 years of the annual cumulated lengths of the bloom

The thermal optimum T_i^{opt} was first defined as the mean minimum temperature of the bloom throughout the whole time series. However, this value led to blooms occuring mainly in the winter and needed to be increased by 5°C in order to simulate realistic phytoplankton cycles.

It should be noted however that a variation in niche width also affects the final shape of thermal preferences. Indeed, when b_i increases, the niche term f_i only encounters small variations in values around the thermal optimum. In this case, the final value of the growth rate is driven by the metabolism part of the equation (Fig. 2).

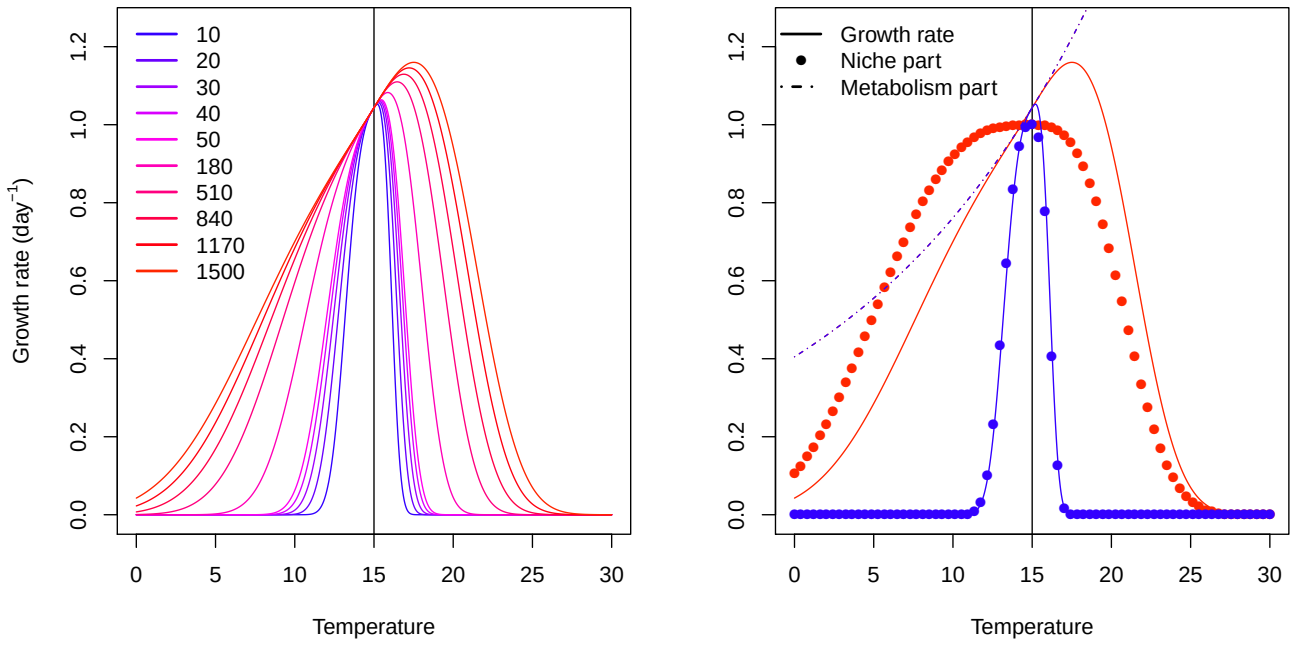

Figure 2: Relationship between daily growth rates and temperature with different values of niche width b (which values are indicated in the legend, corresponding to specialist and generalist taxa) and the same thermal optimum, 15°C, indicated by the solid black line (right). On the left panel, only the two extreme values of b (10 and 1500) are shown in blue and red respectively. Coloured lines then correspond to the final growth rate, points correspond to $f_i(T)$ values (see eq. 1) and dotted lines correspond to $E(T)$ values.

The shift of the maximum growth rate may lead to a deformation of the expected thermal niche of each taxon. We provide actual shapes of $f_i(T)$ for modeled taxa below (Fig XX, TO DO).

Estimation of interactions

Model I: linear interactions

Interactions between taxa have previously been computed with a Multivariate AutoRegressive model (eq. 3, Picoche & Barraquand, 2020).

$$\mathbf{n}_{t+1} = \mathbf{B}\mathbf{n}_t + \mathbf{C}\mathbf{u}_{t+1} + \mathbf{e}_t, \mathbf{e}_t \sim \mathcal{N}_{\mathcal{S}}(0, \mathbf{Q}) \quad (3)$$

where $\mathbf{n}_t$ is the $1 \times S$ vector of log-abundance of phytoplankton taxa, $\mathbf{B}$ is the $S \times S$ interaction matrix with elements b_{ij}, $\mathbf{C}$ is the $S \times V$ environment matrix describing the effects of variables $\mathbf{u}_{t+1}$ on growth rates and the noise $\mathbf{e}_t$ is a $1 \times S$ noise vector following a multivariate normal distribution with a variance-covariance matrix $\mathbf{Q}$.

The interaction model we use in this paper is a Beverton-Holt model (eq. 1).

Certain *et al.* (2018) showed that MAR and BH interaction coefficients, respectively b_{ij} and α_{ij}, could map once abundances at equilibrium N_i^* are defined.

$$\begin{cases} b_{ii} - 1 = & \frac{-\alpha_{ii} N_i^*}{1+\sum_l \alpha_{il} N_l^*} \\ b_{ij, i \neq j} = & \frac{-\alpha_{ij} N_j^*}{1+\sum_l \alpha_{il} N_l^*} \end{cases}$$

Let's define $\tilde{b_{ij}}$ with $\tilde{b_{ii}} = b_{ii} - 1$, and $f_A(i) = \sum_l \alpha_{ij} N_l^*$.

$$\tilde{b_{ij}}(1 + f_A(i)) = -\alpha_{ij} N_j^*$$

We then sum on columns (on j).

$$\sum_j [\tilde{b_{ij}}(1 + f_A(i))] = -f_A(i)$$

$$\Leftrightarrow -f_A(i)(1 + \sum_j \tilde{b_{ij}}) = \sum_j b_{ij}$$

$$\Leftrightarrow f_A(i) = -\frac{\sum_j \tilde{b_{ij}}}{(1 + \sum_j \tilde{b_{ij}})}$$

$$\Leftrightarrow \alpha_{ij} = -\frac{1}{N_j^*} \tilde{b_{ij}} (1 - \frac{\sum_j \tilde{b_{ij}}}{1 + \sum_j \tilde{b_{ij}}})$$

$$\Leftrightarrow \alpha_{ij} = -\frac{1}{N_j^*} \frac{\tilde{b_{ij}}}{1 + \sum_j \tilde{b_{ij}}}$$

This gives an exact correspondance between α_{ij} and b_{ij}.

In this model, the presence of mutualistic interactions can lead to an orgy of mutual benefaction [ref]. We impose a minimum value of 1 to the denominator of the BH formulation, meaning that the growth rate cannot be higher than the maximum growth rate calculated $r_i(T)$. We acknowledge the possibility of overyielding, i.e. an increase in growth due to the presence of other species, but the phenomenon seems quite rare for phytoplanktonic communities (see Schmidtke et al. 2010 for underyielding and see Shurin et al. 2014 for an observed but not frequent, and small, overyielding).

Model II: saturating interactions

We now move to a model with saturating interactions between taxa.

$$N_{t+1,i} = \frac{e^{r_i(T)} N_{t,i}}{1 + \sum_{j/a \in \mathbb{C}} \frac{a_C N_{t,j}}{H_{ij} + N_{t,j}} + \sum_{j/a \in \mathbb{F}} \frac{a_F N_{t,j}}{H_{ij} + N_{t,j}}} \tag{4}$$

where coefficients a_C and a_F are the maximum interaction strength for competition and facilitation respectively, H_{ij} coefficients are the abundance of species j to reach half of the maximum effect in the interaction of j on i,

and $\mathbb{C}$ and $\mathbb{F}$ are the sets of competitive and facilitative interactions. This formula can be linked with the Unique Interaction Model by Qian & Akçay, 2020, i.e. a model where each taxon provides a unique type of benefit or disadvantage to the focus species.

It is easy to see that there is no unique solution for the correspondence between the **B** matrix of the MAR model and the new formulation including H_{ij}, a_C and a_F. We approximate the maximum interaction strength a_C as the average sum of all interactions α_{ij} exerted on a given species if all interactions were competitive (eq. 5). To compute a_F, we can make two assumptions: a) there is 70% facilitation in our dataset and b) the growth rate $r_i(T)$ cannot be exceeded, as in model I (eq. 6).

$$a_C = \frac{1}{S}\sum_i \left(\sum_j \alpha_{ij} N_{j,max} \right) \quad (5)$$

$$(1-0.7)a_C + 0.7a_F = 1 \quad (6)$$

At low abundances, we can consider that interactions are far from saturation. Taking the tangent of the function at this point, H_{ij} can be approximated by $\frac{a_{C/F}}{\alpha_{ij}}$.

Fixed parameters

This section contains additional information of parameter definition, estimation and value.

Loss rate The loss rate corresponds to multiple mortality processes. Scranton & Vasseur (2016) set this rate around 0.04 day^{-1}. In Jewson *et al.* (1981), washout (0.5%), parasitism (4% of infested cells) and grazing still remained low when compared to growth rates. Li *et al.* (2000) found values between 0.02 and 0.1 for natural mortality only, while a review by Sarthou *et al.* (2005) indicates a loss of daily primary productivity between 0.45 and 1.1 due to grazing only, 0.13 being potentially due to cell autolysis (in the absence of nutrients, or because of viral charge). From this overview, the reference values for the models, 0.2, is a trade-off between sometimes high level of mortality and richness conservation in the model.

Sinking rate Among the hydrodynamics processes that drive sinking rate, turbulence and eddies, themselves driven by tidal currents, shape of the estuary or wind conditions, can retain the cells at the top of the water column [ref to Sourisseau?]. This is why lab experiments on sinking rates are not sufficient to calibrate a field-based model. Credible values for sinking rates are therefore taken from field studies. In the Gotland Basin (central Baltic Sea), Passow (1991) measured a large variability in sinking rates, even within the same genus (e.g., between 1 and 30% for *Chaetoceros* spp.). However, a pattern could be distinguished, with a small number of genera that sinked more than the rest of the community. The mean rate for *Chaetoceros* and *Thalassiosira* was around 10% while it was around 1% for the other species. Sinking rate values around 10% are consistent with the loss rate values in Kowe *et al.* (1998) in a river and Wiedmann *et al.* (2016) in an estuary (mouth of Adventfjorden). Variations of the sinking rate over time give values between 4 and 50% (Jewson *et al.*, 1981). The chosen beta-distribution (Fig. S3) therefore accounts for both maximum and mean values, while still allowing a highly skewed distributions. High sinking rates are kept for the morphotypes corresponding to *Chaetoceros* (CHA) and *Thalassiosira* (THP).

However, it should be noted that the sinking rate measured in these articles represent the sinking of all cells, therefore including dead cells. In our model, it should represent the exchange of live cells between the coast and the seed bank, or a loss of cells in the ocean. The maximum sinking rate used in this model might therefore need to be decreased to avoid modeling dead cells already taken into account in the loss term.

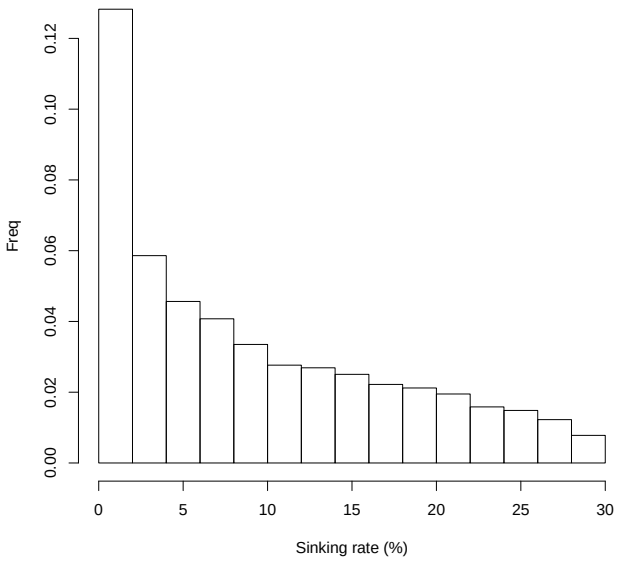

Figure 3: Possible beta-distribution of sinking rates

Cyst mortality McQuoid *et al.* (2002) present maximum and mean depth at which germination of diatoms and dinoflagellates could still occur when incubated. The authors also present sediment datation according to depth. Depth can therefore be related to maximum and mean age of phytoplankton cysts before death.

Assuming m is the probability of mortality, m follows a geometric law, i.e., m is the probability distribution of the number of days needed for a phytoplankon cyst to die. The expectancy for the life duration (the number of days without dying) is $\frac{1}{m} \Leftrightarrow m = \frac{1}{L_{mean}}$where L_{mean} is the average life duration.

Another way to look at the process is that life expectancy L follows the distribution $p(L > l) = e^{-ml}$.With maximum values, we can arbitrarily choose that for these values $p(L > l_{max}) = 0.05$. In this, $m = -\frac{ln(p(L>l_{max}))}{l_{max}}$.

In both cases, $m \propto 10^{-4}\mathrm{d}^{-1}$.

Resuspension As mentioned in the main text, resuspension values are mostly taken from model or data for inorganic particles. Rates vary from one publication to another: in Fransz & Verhagen (1985) in a coastal area, the resuspension rate of sediments is evaluated around 5.10^{-5} day^{-1} in winter and decreases in summer, with a link between resuspension and light extinction coefficient. In Kowe *et al.* (1998), the resuspension rate of diatoms is evaluated around $1.9.10^{-5}$ day^{-1}. In Le Pape *et al.* (1999), resuspension rate of sediments and dead diatoms is 0.002 day^{-1}. In this paper, we explore values between 10^{-5} (stratified water column) to 0.1 (highly mixed environment).

Finally, it should be noted that cyst burial, sinking rate and resuspension are all dependent on the hydrodynamics of the place and are therefore, at least in biological terms, not identifiable.

References

Bissinger, J., Montagnes, D., Harples, J. & Atkinson, D. (2008). Predicting marine phytoplankton maximum growth rates from temperature: Improving on the Eppley curve using quantile regression. *Limnology and Oceanography*, 53, 487–493.

Certain, G., Barraquand, F. & Gåardmark, A. (2018). How do MAR(1) models cope with hidden nonlinearities in ecological dynamics? *Methods in Ecology and Evolution*, 9, 1975–1995.

Edwards, K., Thomas, M., Klausmeier, C. & Litchman, E. (2015). Light and growth in marine phytoplankton: allometric, taxonomic, and environmental variation. *Limnology and Oceanography*, 60, 540–552.

Edwards, K., Thomas, M., Klausmeier, C. & Litchman, E. (2016). Phytoplankton growth and the interaction of light and temperature: A synthesis at the species and community level. *Limnology and Oceanography*, 61, 1232–1244.

Eppley, R. (1972). Temperature and phytoplankton growth in the sea. *Fishery Bulletin*, 70, 1063–1085.

Fransz, H. & Verhagen, J. (1985). Modelling research on the production cycle of phytoplankton in the Southern Bight of the North Sea in relation to riverborne nutrient loads. *Netherlands Journal of Sea Research*, 19, 241–250.

Jewson, D.H., Rippey, B.H. & Gilmore, W.K. (1981). Loss rates from sedimentation, parasitism, and grazing during the growth, nutrient limitation, and dormancy of a diatom crop. *Limnology and Oceanography*, 26, 1045–1056.

Kowe, R., Skidmore, R., Whitton, B. & Pinder, A. (1998). Modelling phytoplankton dynamics in the River Swale, an upland river in NE England. *Science of The Total Environment*, 210, 535–546.

Le Pape, O., Jean, F. & Ménesguen, A. (1999). Pelagic and benthic trophic chain coupling in a semi-enclosed coastal system, the Bay of Brest (France): a modelling approach. *Marine Ecology Progress Series*, 189, 135–147.

Li, M., Gargett, A. & Denman, K. (2000). What determines seasonal and interannual variability of phytoplankton and zooplankton in strongly estuarine systems? *Estuarine, Coastal and Shelf Science*, 50, 467–488.

McQuoid, M.R., Godhe, A. & Nordberg, K. (2002). Viability of phytoplankton resting stages in the sediments of a coastal Swedish fjord. *European Journal Phycology*, 37, 191–201.

Passow, U. (1991). Species-specific sedimentation and sinking velocities of diatoms. *Marine Biology*, 108, 449–455.

Picoche, C. & Barraquand, F. (2020). Strong self-regulation and widespread facilitative interactions between genera of phytoplankton. preprint, bioRxiv.

Qian, J. & Akçay, E. (2020). The balance of interaction types determines the assembly and stability of ecological communities. *Nature Ecology & Evolution*, 4, 356–365.

Reynolds, C.S. (2006). *The ecology of phytoplankton*. Cambridge University Press.

Sarthou, G., Timmermans, K.R., Blain, S. & Tréguer, P. (2005). Growth physiology and fate of diatoms in the ocean: a review. *Journal of Sea Research*, 53, 25–42.

Scranton, K. & Vasseur, D.A. (2016). Coexistence and emergent neutrality generate synchrony among competitors in fluctuating environments. *Theoretical Ecology*, 9, 353–363.

Wiedmann, I., Reigstad, M., Marquardt, M., Vader, A. & Gabrielsen, T. (2016). Seasonality of vertical flux and sinking particle characteristics in an ice-free high arctic fjord-Different from subarctic fjords? *Journal of Marine Systems*, 154, 192–205.